Journal of Nonlinear Science (2023) 33:11
https://doi.org/10.1007/s00332-022-09859-w

Journal of Nonlinear Science

# Modulation Theory for Radially Symmetric Kink Waves Governed by a Multi-Dimensional Sine-Gordon Equation

**Lu Trong Khiem Nguyen**[1] · **Noel Frederick Smyth**[2,3]

Received: 11 October 2021 / Accepted: 30 September 2022


**Abstract**
We derive a modulation theory for the resolution of radially symmetric kink waves governed by a multi-dimensional sine-Gordon equation. Whitham modulation theory is developed to explain the return of an expanding kink wave, as well as predicting its maximum expansion radius and its return time. Comparisons with full numerical solutions of the sine-Gordon equation show that the modulation theory gives excellent predictions for not only the returning time and the maximum expansion radius, but also for the details of the kink itself. In addition, the method can be extended to dissipative sine-Gordon equations and generalized to deal with a wide class of initial conditions beyond kinks.

**Keywords** Returning effect · Sine-Gordon equation · Modulation theory · Kink waves

**Mathematics Subject Classification** 78-10 · 81Txx · 35Qxx

## 1 Introduction

The sine-Gordon equation

$$\frac{\partial^2 u}{\partial t^2} - \frac{\partial^2 u}{\partial x^2} + \sin u = 0 \tag{1}$$

Communicated by Robert Buckingham.

✉ Lu Trong Khiem Nguyen
khiem.nguyen@glasgow.ac.uk

Noel Frederick Smyth
N.Smyth@ed.ac.uk

1 James Watt School of Engineering, University of Glasgow, Glasgow G12 8QQ, Scotland, UK

2 School of Mathematics, University of Edinburgh, Edinburgh EH9 3FD, Scotland, UK

3 School of Mathematics and Applied Statistics, University of Wollongong, Wollongong, NSW 2522, Australia

Published online: 19 November 2022

is one of the standard nonlinear dispersive wave equations which is integrable using the method of inverse scattering (Lamb 1980; Whitham 1974). It arises in a large number of areas of physics, for example, crystal dislocation theory (Lamb 1980), self-induced transparency (Lamb 1980), laser physics (Lamb 1980) and particle physics (Adkins et al. 1983; Kudryavtsev et al. 1998). It is also a special case of the Baby Skyrme model which describes nonlinear baryons (Piette and Zakrzewski 1998). The soliton solution of the sine-Gordon equation is the kink solution

$$u = 4 \arctan e^{\pm \frac{x-Ut}{\sqrt{1-U^2}}}, \tag{2}$$

which is a front solution whose derivative with respect to $x$ has the classic humped-shaped solitary wave profile. Solution (2) represents both kink (a front from 0 to $2\pi$) and anti-kink (a front from $2\pi$ to 0) solutions, depending on the sign.

The one-dimensional sine-Gordon equation is integrable, so that, in principle, its solution is well understood. However, solutions of the higher-dimensional sine-Gordon equation

$$\frac{\partial^2 u}{\partial t^2} - \nabla^2 u + \sin u = 0 \tag{3}$$

are not well understood as the higher-dimensional equation is not integrable, so that its solutions show a much wider range of possible behaviours. For instance, while ring-shaped kink waves are unstable for the two-dimensional sine-Gordon equation, it was proposed that the addition of azimuthal variations could stabilize a radial kink (Neu 1990). However, as the kink evolves, it sheds dispersive radiation and it was subsequently shown that this shed radiation eventually causes the azimuthal variations to decay, so that the kink still eventually collapses (Minzoni et al. 2001). The analysis of kink, or other solitary wave solutions, of the higher-dimensional sine-Gordon equation is difficult. For this reason, variational approximations have proved to be popular, based on suitable trial functions based on the kink solution of the one-dimensional sine-Gordon Eq. (1). Such variational methods were first applied to the nonlinear Schrödinger (NLS) equation (Anderson 1983) and then extended to include the dispersive radiation shed by a solitary wave as it evolves (Kath and Smyth 1995), with excellent agreement found with numerical solutions. Variational methods have subsequently been applied to many nonlinear dispersive wave equations, particularly in nonlinear optics, with excellent results found as long as the trial functions used are appropriately chosen, see the review (Malomed 2002). A variational approximation was developed to examine the evolution of the kink-like initial condition

$$u = 4 \arctan e^{-\frac{x}{w_0}}, \quad \frac{\partial u}{\partial t} = \frac{2U_0}{w_0} \operatorname{sech} \frac{x}{w_0} \tag{4}$$

at $t = 0$ to the exact kink solution as $t$ increases for the one-dimensional sine-Gordon equation (1) (Smyth and Worthy 1999). This initial condition is the exact kink solution if $w_0 = \sqrt{1 - U_0^2}$, see (2). The trial function used was a generalized kink

$$u = 4 \arctan e^{-\frac{x-\xi(t)}{w(t)}}. \tag{5}$$

This trial function was used in a Lagrangian formulation of the sine-Gordon equation to derive modulation equations for the parameters $w(t)$ and $\xi(t)$ (Whitham 1974). These modulation equations were found to give results in excellent agreement with numerical solutions of the sine-Gordon equation with the initial condition (4). This variational method was subsequently extended to study two-dimensional ring-shaped kinks (Minzoni et al. 2001) and breathers (Minzoni et al. 2004).

The present work extends the use of variational methods for the sine-Gordon equation to study the returning effect of multi-dimensional radial kinks governed by the sine-Gordon equation (3) and a damped form of this equation arising in physics, including solid state physics and Josephson transmission lines (Kivshar and Malomed 1989; McLaughlin and Scott 1978). It was found that radially expanding kinks slow down and eventually reverse their propagation direction, returning to the origin and collapsing, termed the returning effect (Christiansen and Olsen 1979; Samuelsen 1979). A slowly varying kink approximation was developed to model this expansion and collapse, which was found to give solutions in excellent agreement with numerical solutions of the sine-Gordon equation, both with and without damping, both for the time evolution of its position and the return time. In addition, initial conditions which were not of the form of one-dimensional kinks were used, an extension of the trial function (5), with excellent agreement with numerical solutions also found.

Modulation equations for one-dimensional and multi-dimensional sine-Gordon equations were developed in Le and Nguyen (2015, 2013), which were used to describe the maximal slope of a packet of well-separated kinks. Indeed, on using a simple wave solution depending on the self-similar variable $\xi = x/t$, it was proved that the maximal slope depends on the kink velocity, which agrees with the slope-velocity relation derived from an exact kink solution. In the case of radially symmetric waves, the theory could justify the returning effect in that the initial positive velocity of the pseudo-kink solution must decrease to zero and then turn negative. The slope-velocity relation remains unchanged after the wave returns. Unfortunately, the returning time, as well as the maximum expansion radius, could not be computed in these works because the initial conditions, namely the initial shape and initial velocity of the wave, were not taken into account. Even when the initial conditions were supplied, it is not easy to incorporate them into the simple wave solutions as the simple wave solution depends on $x/t$, which is singular initially. Additionally, the full resolution of the ring-shaped kink waves was not derived in Le and Nguyen (2015, 2013). In the present work, we derive modulation equations to model the full propagation process of a kink wave for kink-type initial conditions. In addition, the returning time and the maximum expansion radius are found, with excellent agreement with full numerical solutions found.

The higher-dimensional sine-Gordon-type equation studied in the present work is

$$u_{tt} + \beta u_t - \nabla^2 u + \sin u = 0, \tag{6}$$

where $\nabla^2 = \partial_x^2 + \partial_y^2$ is the two-dimensional and $\nabla^2 = \partial_x^2 + \partial_y^2 + \partial_z^2$ the three-dimensional Laplacian, respectively, and $\beta \geq 0$ is the damping coefficient. This equation is a standard model of a damped dc-driven long Josephson current density (see Kivshar and Malomed (1989); McLaughlin and Scott (1978)). Without damp-

ing, namely $\beta = 0$, this sine-Gordon equation is energy conserving, so that it has an associated variational formulation.

## 2 Modulation Theory for Multi-Dimensional Sine-Gordon Equation

As in the previous work of Christiansen and Olsen (1979), the initial condition used for the study of the evolution and return of kink solutions for the sine-Gordon equation (6) is based on the one-dimensional kink solution of the sine-Gordon equation (1). We then use the initial condition

$$\begin{aligned} u(\mathbf{x}, 0) &= u_0(\mathbf{x}) = 4 \arctan\left[ \exp\left( \frac{r - R_0}{w_0} \right) \right], \\ u_t(\mathbf{x}, 0) &= v_0(\mathbf{x}) = \frac{2c_0}{w_0} \operatorname{sech}\left( \frac{r - R_0}{w_0} \right), \quad r = \|\mathbf{x}\|, \end{aligned} \tag{7}$$

where $w_0$, $c_0$ and $R_0$ are constants. This radially symmetric kink $u = u(\|\mathbf{x}\|, t)$ will be termed a ring-shaped kink. The parameter $R_0$ corresponds to the initial position of the kink, $c_0$ to its initial velocity and $w_0$ to its initial width. Our goal is to obtain the evolution of this initial condition for the sine-Gordon equation (6) in both two and three dimensions. As the initial condition (7) is radially symmetric, the kink solution $u = u(r, t)$ is radially symmetric and the sine-Gordon equation becomes

$$u_{tt} + \beta u_t - u_{rr} - \frac{d-1}{r} u_r + \sin u = 0, \tag{8}$$

where $d = 2, 3$ is the number of spatial dimensions.

Let us now consider the derivation of Whitham modulation theory for the kink solution of the sine-Gordon equation (3), noting that this equation is (8) with $\beta = 0$. In standard Whitham modulation theory, the modulated solution $u = u(\theta(\mathbf{x}, t))$ is assumed to be periodic in $\theta$, with the phase variable $\theta$ the fast variable, while the wave parameters, such as the wave number $\mathbf{k} = \nabla\theta$, the wave frequency $\omega = -\theta_t$ and the amplitude $A = \max u - \min u$, are slow variables which modulate the wave envelope, see Whitham (1965, 1974). Indeed, upon substituting the solution form $u = u(\theta)$ into (6), we obtain the ODE for the periodic wave solution

$$\frac{1}{2}(\omega^2 - \mathbf{k}\cdot\mathbf{k}) u_\theta^2 + 1 - \cos u = E, \tag{9}$$

where $E$ is an integration constant representing the initial energy of the system. The phase plane for this equation is shown in Fig. 1. Focussing on the periodic region, it is clear that the periodic wave solution is bounded between two constants in the interval $[0, 2\pi]$. The kink solution, just like the soliton solution of the KdV equation, is achieved in the limit in which $u$ increases from 0 to $2\pi$ and is trapped at this level. This is the key consideration in deriving the slope modulation solutions of Le and Nguyen (2015, 2013). When the periodic solution $u = u(\theta)$ tends to the kink-type solution, the period of the solution tends to infinity. Let us consider the periodic

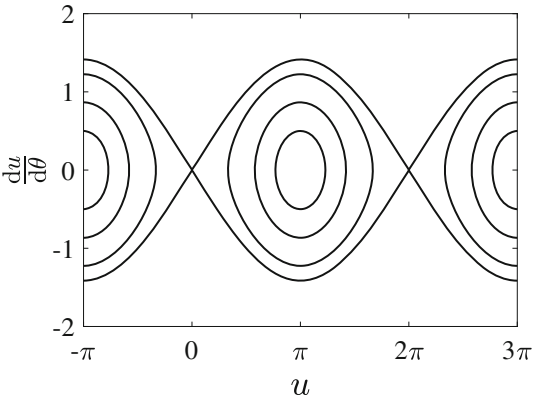


**Fig. 1** Phase contours in the $(u, u_\theta)$-plane for the conserved energy (9). Here, $m = \omega^2 - \mathbf{k}\cdot\mathbf{k} = 1$. Periodic waves correspond to closed contours and the kink to the limiting case with the contour $\frac{1}{2}u_\theta^2 + \cos u - 1 = 0$

solution $u = u(\theta(r,t))$ in $\theta$, with $r = \|\mathbf{x}\|$ being the radial coordinate. On fixing the time $t$, the phase variable $\theta$ varies with the spatial coordinate $r$. As the kink solution has infinite period, averaging over the phase variable $\theta$ can be replaced with averaging over the entire spatial domain (Whitham 1974), which is how the averaged Lagrangian density and the averaged dissipation density are defined in the next sections.

Whitham modulation theory is based on a slowly varying (exact) periodic wave solution of the underlying equation. Then, standard Whitham modulation theory cannot be used for general initial conditions of the form (7), unless $w_0 = \sqrt{1 - c_0^2}$ in the one-dimensional case, so that the initial condition is an exact sine-Gordon equation kink. In higher dimensions, there are no known exact kink solutions on which to base Whitham modulation theory. To extend the technique of modulation theory to initial conditions which are not exact solutions of the relevant nonlinear dispersive wave equation, Anderson (1983) used suitable trial functions, mimicking the solitary wave solution, in a variational formulation of the governing equation. This approach has been extended to the sine-Gordon equation in one and two dimensions (Minzoni et al. 2001; Smyth and Worthy 1999). To this end, we assume that the solution has the shape of a radially symmetric kink of the form

$$u(r,t) = 4\arctan\left[\exp(\theta(r,t))\right], \quad \theta(r,t) = \frac{r - R(t)}{w(t)}, \tag{10}$$

where $R(t)$ and $w(t)$ are the position and the width of the kink. This trial function is a (slowly) varying solitary wave based on the one-dimensional sine-Gordon kink with time-dependent position and width. These varying parameters are determined from the modulation equations derived from the Lagrangian formulation of the sine-Gordon equation. As a kink has an infinite period, the modulation equations are obtained by averaging over the spatial coordinate $r$ from $r = 0$ to $r = +\infty$ (Anderson 1983; Whitham 1974). Taking the derivative of the trial function (10), we obtain

$$u_r = \frac{2}{w(t)}\operatorname{sech}\left(\frac{r - R(t)}{w(t)}\right), \quad u_t = -\frac{2}{w(t)^2}\operatorname{sech}\left(\frac{r - R(t)}{w(t)}\right)[a(t)r + b(t)], \tag{11}$$

where

$$a(t) = w'(t), \quad b(t) = w(t)R'(t) - R(t)w'(t) \tag{12}$$

and primes denote derivatives with respect to $t$.

### 2.1 Modulation Equations

To derive Whitham modulation equations for the multi-dimensional sine-Gordon equation (6), we average out the fast variations in the Lagrangian formulation for this equation to obtain variational equations for the slow variables $R(t)$ and $w(t)$. The sine-Gordon equation (6) is the stationary point of the variational problem for the Lagrangian $L$ and the dissipation density $D$

$$L(u_t, \nabla u, u) = \frac{1}{2}u_t^2 - \frac{1}{2}\nabla u \cdot \nabla u - \phi(u), \quad \phi(u) = 1 - \cos u, \quad D(u_t) = \frac{1}{2}\beta(u_t)^2. \tag{13}$$

The second term is formally added to include loss into the system. Indeed, the Euler-Lagrange equation

$$\frac{\partial L}{\partial u} - \frac{\partial}{\partial t}\frac{\partial L}{\partial u_t} - \nabla \cdot \frac{\partial L}{\nabla u} - \frac{\partial D}{\partial u_t} = 0 \tag{14}$$

gives the sine-Gordon Eq. 6. As the trial function (10) is radially symmetric, the variational formulation of the sine-Gordon Eq. (6) simplifies to

$$\begin{aligned} \delta \int_t \kappa \int_0^\infty \left[\frac{1}{2}u_t^2 - \frac{1}{2}u_r^2 - (1 - \cos u)\right] r^{d-1}\, \mathrm{d}r\mathrm{d}t \\ - \int_t \kappa \int_0^\infty \beta \left[u_t \frac{\partial u}{\partial R}\delta R + u_t \frac{\partial u}{\partial w}\delta w\right] r^{d-1}\, \mathrm{d}r\mathrm{d}t = 0, \end{aligned} \tag{15}$$

where $d = 2$ and $\kappa = 2\pi$ for the 2D ring-shaped waves and $d = 3$ and $\kappa = 2\pi^2$ for 3D waves. As the constant $\kappa$ can be factored out, we drop it before deriving the averaged Lagrangian and the averaged dissipation density.

### 2.2 Averaged Lagrangian and Averaged Dissipation Density

Following (15), we define the Lagrangian for radially symmetric waves in 2D ($d = 2$) and 3D ($d = 3$) as

$$\mathcal{L}_d(u_t, u_r, u) = \int_0^\infty \left[\frac{1}{2}u_t^2 - \frac{1}{2}u_r^2 - (1 - \cos u)\right] r^{d-1}\, \mathrm{d}r, \quad d = 2, 3. \tag{16}$$

Similarly, to derive the modulation equations for $R = R(t)$ and $w = w(t)$, we also determine the averaged dissipation density via two components

$$\mathcal{D}_d^R = \beta \int_0^\infty u_t \frac{\partial u}{\partial R} r^{d-1} \mathrm{d}r, \quad \mathcal{D}_d^w = \beta \int_0^\infty u_t \frac{\partial u}{\partial w} r^{d-1} \mathrm{d}r. \tag{17}$$

First, let us focus on calculating the average of the Lagrangian $L$, $\mathcal{L}_d$. Substituting the solution ansatz (10) and its derivatives (11) into the Lagrangian and averaging it by integrating in $r$ from 0 to $\infty$ (Whitham 1974), we find $\mathcal{L}_d$ in terms of $R(t)$ and $w(t)$ as

$$\begin{aligned}\mathcal{L}_d(R, w, R', w') = \frac{2}{w^4}\Big[a(w')^2 G_{d+1}(R, w) + 2a(w')b(R, w, R', w')\, G_d(R, w)\\ + b(R, w, R'w')^2 G_{d-1}(R, w)\Big] - \Big(\frac{2}{w^2} + 1\Big)G_{d-1}(R, w),\end{aligned} \tag{18}$$

where

$$G_j(R, w) = \int_0^\infty r^j \operatorname{sech}^2\left(\frac{r - R}{w}\right) \mathrm{d}r, \quad j = 1, \ldots, 4. \tag{19}$$

The expressions for the integrals $G_j$ are involved, so they are derived and presented in detail in Appendix 1. The end result is

$$\begin{aligned} G_1(R, w) &= -w^2 P_1\Big[-\exp\left(\frac{2R}{w}\right)\Big], \quad G_2(R, w) = -w^3 P_2\Big[-\exp\left(\frac{2R}{w}\right)\Big],\\ G_3(R, w) &= -\frac{3}{2}w^4 P_3\Big[-\exp\left(\frac{2R}{w}\right)\Big], \quad G_4(R, w) = -3w^5 P_4\Big[-\exp\left(\frac{2R}{w}\right)\Big],\end{aligned} \tag{20}$$

where $P_n(z)$ is the polylogarithm function defined as the convergent series

$$P_n(z) = \sum_{k=1}^{\infty} \frac{z^k}{k^n} < \infty. \tag{21}$$

To complete the modulation equations, we need to calculate the average of the loss term $D$, which is given explicitly by the second integral in (15). The details of this averaging are again given in Appendix 1, with the final result being

$$\begin{aligned}\mathcal{D}_d^R(R, w, R', w') &= \beta\frac{4}{w^3}\big[a(w')\, G_d(R, w) + b(R, w, R', w')\, G_{d-1}(R, w)\big],\\ \mathcal{D}_d^w(R, w, R', w') &= \beta\frac{4}{w^4}\big[a(w')G_{d+1}(R, w) + (b(R, w, R', w') - a(w')R)G_d(R, w)\\ &\quad - b(R, w, R', w')RG_{d-1}(R, w)\big].\end{aligned} \tag{22}$$

### 2.3 Modulation Equations

Taking variations of the averaged Lagrangian (15) with respect to $R(t)$ and $w(t)$ gives the Euler-Lagrange, modulation, equations

$$\begin{aligned}\frac{\mathrm{d}}{\mathrm{d}t}\frac{\partial \mathcal{L}_d}{\partial R'} - \frac{\partial \mathcal{L}_d}{\partial R} + \mathcal{D}_d^R = 0 \quad \text{for } \delta R,\\ \frac{\mathrm{d}}{\mathrm{d}t}\frac{\partial \mathcal{L}_d}{\partial w'} - \frac{\partial \mathcal{L}_d}{\partial w} + \mathcal{D}_d^w = 0 \quad \text{for } \delta w.\end{aligned} \tag{23}$$

As these equations (23) are involved, they need to be solved numerically. After computing the partial derivatives of $\mathcal{L}_d$ with respect to its argument and substituting them into the variational equations (23), we arrive at the modulation equations describing the evolution of the initial condition (7).

To reduce the length of the modulation equations derived from the averaged Lagrangians of Appendix 1, we denote

$$S(t) = \tanh\left[\frac{R(t)}{w(t)}\right] + 1, \quad Q(t) = e^{\frac{2R(t)}{w(t)}} + 1. \tag{24}$$

Then, the Euler-Lagrange Eqs. (23) become
For 2D waves:

$$\begin{aligned}
\delta R : 0 = {} & \frac{2}{w}\left[P_2(1-Q)\left[\left(w'\right)^2 - 2ww''\right] + 2\ln(Q)\left(wR'' - Rw''\right)\right] \\
& + \frac{2}{w^3}S\left[w^2(1+R^2+w^2) + R^2w'(w'-2w)\right] + \mathcal{D}_2^R, \\
\delta w : 0 = {} & \frac{1}{Qw^4}\Big\{2Qw^2P_2(1-Q)\left[-2w^2R'' + 4Rww'' - 2Rww' + R\left(w'\right)^2\right] \\
& - 6Qw^4P_3(1-Q)w'' - 4QRw^3\ln(Q)R'' + 4QR^2w^2\ln(Q)w'' \\
& - 4(Q-1)Rw^2(1+R^2+w^2) + 8R^2ww'\left[(Q-1)R - Qw\ln(Q)\right] \\
& + 4R^2\left(w'\right)^2\left[R - QR + Qw\ln(Q)\right] + 4Qw^3\ln(Q)(R^2+w^2)\Big\} + D_2^w
\end{aligned} \tag{25}$$

For 3D waves:

$$\begin{aligned}
\delta R : 0 = {} & \frac{1}{w^2}\Big\{4wP_2(1-Q)\left[w\left(Rw'' - wR''\right) + R\left(w'\right)^2 - Rww'\right] \\
& - 6w^3P_3(1-Q)w'' + 4w^2\ln(Q)(1+R^2+w^2) \\
& - 8R^2ww'\ln(Q) + 4R^2\ln(Q)\left(w'\right)^2\Big\} + \mathcal{D}_3^R \\
\delta w : 0 = {} & \frac{1}{w^3}\Big\{6w^2P_3(1-Q)\left[w\left(wR'' - 2Rw''\right) - 2R(w')^2 + 2Rww'\right] \\
& + 2wP_2(1-Q)\left[w(3R^2w + 3w^3 + w)\right. \\
& \left. + R\left(2w(Rw'' - wR'') + 5R\left(w'\right)^2 - 8Rww'\right)\right] \\
& + 6w^3P_4(1-Q)[2ww'' + (w')^2] + 4R^3\ln(Q)\left(w'\right)^2 \\
& - 8R^3ww'\ln(Q) + 4Rw^2\ln(Q)(1+R^2+w^2)\Big\} + \mathcal{D}_3^w
\end{aligned} \tag{26}$$

Note that, $P_j(1-Q)$ in the above two systems denote the polylogarithm of $1-Q = -\exp(2R/w)$, not the multiplication between $P_j$ and $1-Q$.

Comparing the initial condition (7) with the trial function (10), we find the initial conditions for the kink position $R$ and width $w$ as

$$R(0) = R_0, \quad R'(0) = c_0, \quad w(0) = w_0, \quad w'(0) = 0. \tag{27}$$

The initial condition used in previous work (Christiansen and Olsen 1979; Samuelsen 1979) was based on the initial width and velocity being linked by the one-dimensional kink relation $w_0 = \sqrt{1 - c_0^2}$. Note also that this relation is consistent with the assumption $v(t) = R'(t)$ used in the work (Samuelsen 1979). The present work generalizes the range of initial conditions used by breaking this connection between the initial width and velocity. Indeed, it is found in the present work that even if the relation $w_0 = \sqrt{1 - c_0^2}$ holds initially, as the kink evolves this relation ceases to be valid, so that $w(t) \neq \sqrt{1 - [R'(t)]^2}$. The modulation theory derived herein then provides an improved approximation over the original work of Samuelsen (1979), particularly for the general case for which $w_0 \neq \sqrt{1 - c_0^2}$. We can then interpret the initial condition (27) as follows: The kink initially propagates with the velocity $c_0$ with the width of the kink determined by $w_0$. The modulation equations (23) with the initial conditions (27) were solved by using the `NDSolve` function available as a built-in function in MATHEMATICA (Wolfram Research 2020).

### 2.4 Numerical Solution of the Modulation Equations

The modulation solutions shown in Fig. 9 give that the position $R(t)$ of the kink reaches a finite maximum and then decreases, while the width $w(t)$ fluctuates in time. The maximum radial expansion $R_{\max}$ can be determined by the time $t_r$ for which $R'(t_r) = 0$. Figure 2 shows this evolution and return of the kink as given by the modulation solution, in both two and three dimensions. The evolution to a maximum radius and the return is clear. As noted above, kink evolution in two and three dimensions is broadly similar.

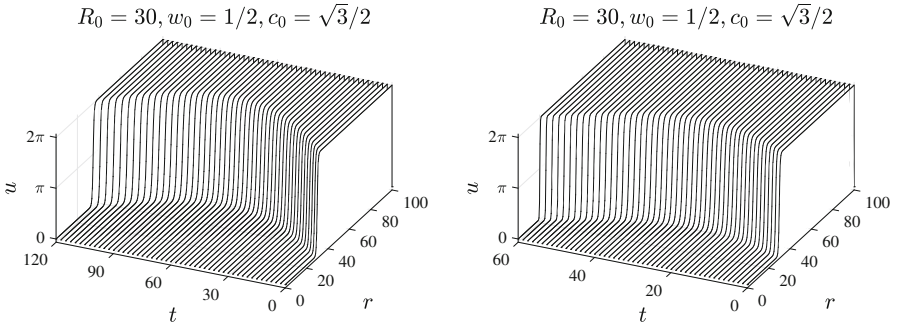


**Fig. 2** Evolution of radially symmetric kink as given by modulation theory: (left) for 2D equation, (right) for 3D sine-Gordon equations

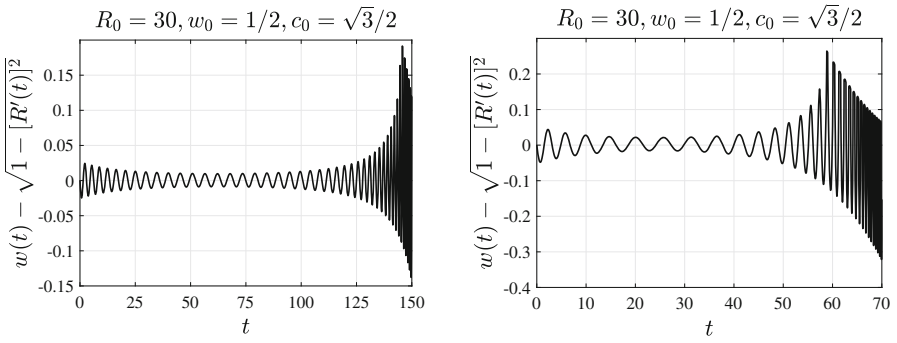


**Fig. 3** The difference $w(t) - \sqrt{1-[R'(t)]^2}$: (left) for 2D equation, (right) for 3D sine-Gordon equations

Figure 3 displays the difference $w(t) - \sqrt{1-[R'(t)]^2}$ for the ring-shaped kinks in both two and three dimensions. It can be seen that $w(t) \approx \sqrt{1-[R'(t)]^2}$ over a rather large time period before the wave returns and then collapses at the origin $r = 0$. This result shows that the relation $w(t) = \sqrt{1-[R'(t)]^2}$ assumed in Samuelsen (1979) is only approximate. Near the point of collapse, and after, the present modulation theory does not hold as the trial function (10) is not an adequate approximation to the solution and breaks down. The study of the behaviour of ring waves upon collapse in the neighbourhood of $r = 0$ is beyond the scope of this work, but deserves further investigation. The key issue is a suitable approximation to the behaviour of the solution near and after collapse. Such a suitable trial function is not clear.

## 3 Numerical Scheme for Sine-Gordon Equation

Before comparing modulation solutions with full numerical solutions of the sine-Gordon equation (6), we briefly discuss the numerical scheme used for the sine-Gordon equation. This numerical scheme is based on using a finite element procedure and the Newton–Raphson method. In particular, for the finite element procedure, we use the variational formulation with time discretization, but without spatial discretization, so that the procedure can be implemented using any high-order finite element method. For the numerical solutions, linear finite elements were used.

The boundary condition

$$\nabla u \cdot \mathbf{n} = 0 \quad \text{on } \partial\Omega \times [0, T] \tag{28}$$

is used for the numerical scheme, where $\partial\Omega$ denotes the boundary of the numerical domain $\Omega$, $\mathbf{n}$ is the outward unit normal vector to the boundary $\partial\Omega$ and $T$ is the maximum simulation time. The Neumann boundary condition (28) was chosen so that the system with $\beta = 0$ conserves the energy

$$E(t) = \int_\Omega \left( \frac{1}{2} u_t^2 + \frac{1}{2} \nabla u \cdot \nabla u + 1 - \cos u \right) \mathrm{d}V.$$

This boundary condition is convenient for the comparisons of the present work as the modulation solutions are valid on an infinite spatial domain, while the numerical solutions are obtained on a finite domain. This ensures that the solutions derived from both methods are energetically equivalent. To match with the modulation theory, the initial conditions (7) are used. To be explicit, we develop herein the numerical procedure for solving the axisymmetric sine-Gordon equation (8) on a one-dimensional domain $\Omega = [a, b]$ instead of the general, multi-dimensional equation (6). The boundary conditions consistent with (28) in this case are $u_r(a) = u_r(b) = 0$.

### 3.1 Weak Form

At a given time instant $t$, multiplying the radially symmetric sine-Gordon equation (8) by $\delta u \in H^1(\Omega)$, applying integration by parts for the term $u_{rr}\delta u$ and the boundary condition $u_r(a) = u_r(b) = 0$, we arrive at

$$\int_\Omega [u_{tt}\delta u + \beta u_t \delta u + u_r \delta u_r + \sin(u)\delta u]\ \mathrm{d}r = 0, \quad \forall \delta u \in H^1(\Omega), \tag{29}$$

where $H^1(\Omega)$ is the Sobolev space of functions defined on $\Omega$. The finite element solution is based on this variational formulation of the radially symmetric sine-Gordon equation (8). In the present work, we examine the propagation of waves before the waves interact with the numerical domain boundary. Next, we need to discretize the above variational equation in time so that the primary variable is the displacement $u$ at a specific time instant $t$. That is, after the time discretization, we seek $u(r, t)$ as a function of $r$, with $t$ considered as fixed.

### 3.2 Time Discretization

Let us assume that $f = f(\mathbf{x}, t)$ is a generic function of $\mathbf{x}$ and $t$. Then, we define $f^t$ as a function of $f$ evaluated at time $t$ with differentiation of $f$ with respect to $t$ denoted by $\dot{f}$. We may then write

$$f^t(\mathbf{x}) = f(\mathbf{x}, t), \quad \dot{f}^t(\mathbf{x}) = \frac{\partial f}{\partial t}(\mathbf{x}, t).$$

Let us partition the time domain $[0, T]$ into $M + 1$ equidistant time steps $t_0, t_1, \ldots t_M$ based on the time step $\Delta t$, i.e. $t_{i+1} - t_i = \Delta t$ for all $i = 0, \ldots, M - 1$. We now solve equation (29) at a given time and therefore require a time discretization formulation. To this end, we employ the trapezoidal rule (or second-order Runge–Kutta method)

$$\begin{aligned} u^{t+\Delta t} &= u^t + \frac{\Delta t}{2}\left(\dot{u}^t + \dot{u}^{t+\Delta t}\right), \\ \dot{u}^{t+\Delta t} &= \dot{u}^t + \frac{\Delta t}{2}\left(\ddot{u}^t + \ddot{u}^{t+\Delta t}\right), \end{aligned} \tag{30}$$

where $u$, $\dot{u}$ and $\ddot{u}$ correspond to the displacement, velocity and acceleration, respectively. These equations mean that the acceleration is linear in the time interval $(t, t+\Delta t)$. Equation (30) can be resolved for $\dot{u}^t$ and $\dot{u}^{t+\Delta t}$ to give

$$\begin{aligned} \dot{u}^t &= \frac{1}{\Delta t}\left(u^{t+\Delta t} - u^t\right) - \frac{\Delta t}{4}\left(\ddot{u}^t + \ddot{u}^{t+\Delta t}\right), \\ \dot{u}^{t+\Delta t} &= \frac{1}{\Delta t}\left(u^{t+\Delta t} - u^t\right) + \frac{\Delta t}{4}\left(\ddot{u}^t + \ddot{u}^{t+\Delta t}\right). \end{aligned} \tag{31}$$

Substitution of Eq. $(31)_2$ for $\dot{u}^{t+\Delta t}$ into Eq. $(30)_2$ now gives

$$\ddot{u}^{t+\Delta t} = \frac{4}{\Delta t^2}\left(u^{t+\Delta t} - u^t\right) - \frac{4}{\Delta t}\dot{u}^t - \ddot{u}^t. \tag{32}$$

Finally, substituting this expression into the weak form (29) evaluated at time $t+\Delta t$, we obtain

$$\begin{aligned} \int_\Omega \Bigg\{ \left[ \left( \frac{4}{\Delta t^2} + \beta \frac{2}{\Delta t} \right)\left(u^{t+\Delta t} - u^t\right) - \left( \frac{4}{\Delta t} + \beta \right)\dot{u}^t - \ddot{u}^t \right]\delta u \\ - \frac{d-1}{r} u_r^{t+\Delta t}\delta u + u_r^{t+\Delta t}\delta u_r + \sin\left(u^{t+\Delta t}\right)\delta u \Bigg\} \, \mathrm{d}r = 0 \end{aligned} \tag{33}$$

for all $\delta u \in H^1(\Omega)$. We solve this *incremental variational equation* for $u^{t+\Delta t}$, the solution at time $t+\Delta t$, given the solution at the last time step, including $u^t$, $\dot{u}^t$ and $\ddot{u}^t$.

***Remark*** On using the trapezoidal rule (30), the scheme is equivalent to the well-known Newmark-$\beta$ method with $\beta = 1/2$; see, e.g. (Bathe 2014).

### 3.3 Linearization and Numerical Algorithm

The incremental variational equation (33) can be set in the form

$$G(u^{t+\Delta t}, \delta u) = F(\delta u), \quad \forall \delta u, \tag{34}$$

where

$$\begin{aligned} G(u^{t+\Delta t}, \delta u) &= \int_\Omega \left\{ \left( \frac{4}{\Delta t^2} + \beta \frac{2}{\Delta t} \right) u^{t+\Delta t}\delta u - \frac{d-1}{r} u_r^{t+\Delta t}\delta u + u_r^{t+\Delta t}\delta u_r \right. \\ &\quad \left. + \sin\left(u^{t+\Delta t}\right)\delta u \right\} \mathrm{d}r, \\ F(\delta u) &= \int_\Omega \left\{ \left( \frac{4}{\Delta t^2} + + \beta \frac{2}{\Delta t} \right) u^t + \left( \frac{4}{\Delta t} + \beta \right)\dot{u}^t + \ddot{u}^t \right\} \delta u \, \mathrm{d}r. \end{aligned} \tag{35}$$

As Eq. (34) is linear in $\delta u$ and nonlinear in $u^{t+\Delta t}$, we solved it for $u^{t+\Delta t}$ using the Newton–Raphson method. To this end, a linearization of it with respect to $u^{t+\Delta t}$ was

required. We compute the directional derivative of $G(u, \delta u)$ with respect to the first argument $u$ in the direction $\Delta u \in H^1(\Omega)$ as follows:

$$\begin{aligned}\left\langle D_u G(u, \delta u), \Delta u \right\rangle &= \int_\Omega \left\{ \left( \frac{4}{\Delta t^2} + \beta \frac{2}{\Delta t} \right) \Delta u \, \delta u - \frac{d-1}{r} \Delta u_r \delta u \right. \\ &\quad \left. + \Delta u_r \delta u_r + \cos(u) \Delta u \, \delta u \right\} \mathrm{d}r. \end{aligned} \tag{36}$$

The superscript $t + \Delta t$ on $u$ has been dropped as it is irrelevant in equation (36). The Newton-Raphson iteration is then

$$\begin{aligned}\left\langle D_u G(u^{t+\Delta t,[n]}, \delta u), \Delta u^{t+\Delta t,[n]} \right\rangle &= F(\delta u) - G(u^{t+\Delta t,[n]}, \delta u), \quad \forall \delta u \in H^1(\Omega), \\ u^{t+\Delta t,[n+1]} &= u^{t+\Delta t,[n]} + \Delta u^{t+\Delta t,[n]} \end{aligned} \tag{37}$$

for all $n$ until the convergence criterion is achieved. As the directional derivative $\langle D_u G(u, \delta u), \Delta u \rangle$ is not only linear in $\delta u$, but also in $\Delta u$, equation $(37)_1$ is a linear equation for $\Delta u^{t+\Delta t,[n]}$. As for the convergence criterion, we ensured that the $L^2$-norm of the residual vector corresponding to the spatial discretization of the right-hand side of $(37)_1$ is smaller than the tolerance $\mathrm{TOL} = 10^{-6}$.

We now decompose the computational domain $\Omega$ into $N_{\mathrm{elem}}$ elements $\Omega^{(e)}$, $e = 1, \ldots, N_{\mathrm{elem}}$, such that

$$\bigcup_{e=1}^{N_{\mathrm{elem}}} \Omega^{(e)} = \Omega \quad \text{and} \quad \Omega^{(m)} \cap \Omega^{(n)} = \emptyset, \quad \forall m \neq n,$$

and rewrite equation $(37)_1$ as follows:

$$\begin{aligned}&\sum_{e=1}^{N_{\mathrm{elem}}} \int_{\Omega^{(e)}} \left\{ \left( \frac{4}{\Delta t^2} + \beta \frac{2}{\Delta t} \right) \Delta u^{t+\Delta t,[n]} \delta u - \frac{d-1}{r} \Delta u_r^{t+\Delta t,[n]} \delta u \right. \\ &\quad \left. + \Delta u_r^{t+\Delta t,[n]} \delta u_r + \cos\left(u^{t+\Delta t,[n]}\right) \Delta u_r^{t+\Delta t,[n]} \delta u \right\} \mathrm{d}r \\ &= \sum_{e=1}^{N_{\mathrm{elem}}} \left[ \int_{\Omega^{(e)}} \left\{ \left( \frac{4}{\Delta t^2} + \beta \frac{2}{\Delta t} \right) u^t + \left( \frac{4}{\Delta t} + \beta \right) \dot{u}^t + \ddot{u}^t \right\} \delta u \, \mathrm{d}r \right. \\ &\quad - \int_{\Omega^{(e)}} \left\{ \left( \frac{4}{\Delta t^2} + \beta \frac{2}{\Delta t} \right) u^{t+\Delta t,[n]} \delta u - \frac{d-1}{r} u_r^{t+\Delta t,[n]} \delta u \right. \\ &\quad \left. \left. + u_r^{t+\Delta t,[n]} \delta u_r + \sin(u^{t+\Delta t,[n]}) \delta u \right\} \mathrm{d}r \right]. \end{aligned} \tag{38}$$

Note that, this iterative scheme is in a continuous setting in that the spatial discretization has not been specified yet. At this point, any conforming high-order finite element method can be used to find the numerical solution of the sine-Gordon equation. The numerical scheme (38) was used for comparisons between the modulation and full

numerical solutions of the sine-Gordon equation. In particular, these full numerical solutions confirm the expansion, return and collapse of the kink.

## 4 Comparison of Modulation Theory With Numerical Solutions

### 4.1 Previous Results

Firstly, we shall consider the specific case for which the initial condition (7) is of the form of a 1D sine-Gordon equation kink with $w_0^2 = 1 - c_0^2$. The results of the previous work (Samuelsen 1979) can be summarized as follows. The initial condition

$$u(r,t) = 4\arctan\left[\exp\left(\frac{r - R(t)}{\sqrt{1 - v^2(t)}}\right)\right] \tag{39}$$

was assumed, with $v(t) = R'(t)$. By using conservation of total energy, the solution $R = R(t)$ was obtained as

$$\begin{aligned} R &= R_{\max}\cos\left(\frac{t - t_r}{R_{\max}}\right) && \text{for 2D,} \\ R &= R_{\max}\mathrm{cn}\left(\sqrt{2}\,\frac{t - t_r}{R_{\max}};\,\frac{1}{2}\right) && \text{for 3D,} \end{aligned} \tag{40}$$

where $\mathrm{cn}(z;m)$ is the Jacobi elliptic cosine function of modulus $m$. These relations give the position $R = R(t)$ of the kink as long as $R_{\max}$ and $t_r$ are known. The parameters $R_{\max}$ and $t_r$ are then, following Samuelsen (1979), given by

$$\begin{aligned} R_{\max} &= \frac{R_0}{(1-c_0^2)^{1/2}}, \qquad t_r = \frac{R_0}{\sqrt{1-c_0^2}}\arccos\left(\sqrt{1-c_0^2}\right) && \text{for 2D,} \\ R_{\max} &= \frac{R_0}{(1-c_0^2)^{1/4}}, \qquad t_r = \frac{1}{\sqrt{2}}\frac{R_0}{(1-c_0^2)^{1/4}}\mathrm{F}\left(\frac{1}{2}, \arccos\left[(1-c_0^2)^{1/4}\right]\right) && \text{for 3D,} \end{aligned} \tag{41}$$

where $F$ denotes the elliptic integral of the first kind. The expression for $u(r,t)$ is obtained by substituting the solution (40) with the parameters $R_{\max}$ and $t_r$ defined by (41) into the solution ansatz (39). This then gives the modulation solution for the full evolution of the kink.

***Remark*** The above results are for the sine-Gordon equation without viscosity, i.e. $\beta = 0$. Note that, the expression for $t_r$ for the 3D case, namely the second of $(41)_2$, differs from its counterpart reported in Samuelsen (1979). After careful recalculation, we found that the argument $z$ in the elliptic integral $F(z,\cdot)$ should be $1/2$ instead of $\pi/4$ as given by (41). With this correction, the agreement between modulation theory, existing results (41) and numerical solutions is excellent, confirming our correction of $t_r$.

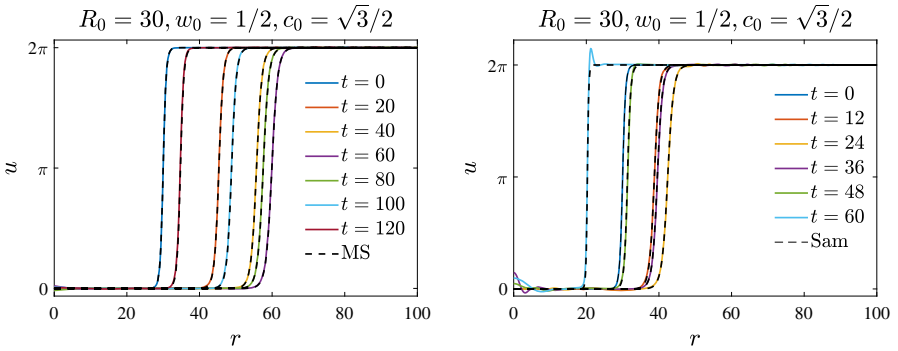


**Fig. 4** Comparison between full numerical solutions and solutions obtained by the heuristic approach (Samuelsen 1979): (left) 2D, (right) 3D sine-Gordon equations. The legend "Sam" denotes the solution obtained by using Samuelsen's result (Samuelsen 1979)

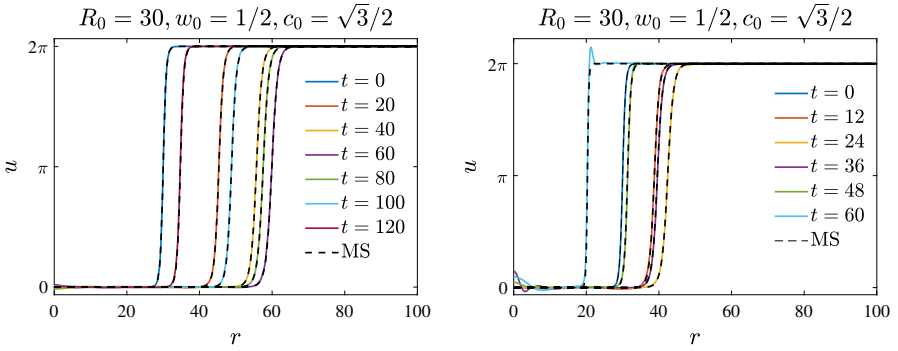


**Fig. 5** Comparison between direct numerical solutions and modulation solutions of the present work: (left) 2D, (right) 3D sine-Gordon equations. The coloured lines present the numerical solution and the dashed lines correspond to modulation solutions

Comparisons between the modulation solution of Samuelsen (1979) and full numerical solutions are shown in Fig. 4. The numerical solution is shown by the full coloured lines and the modulation solution by the dashed lines. It can be seen that there is nearly exact agreement between the modulation and numerical solutions, up until collapse is reached. Near collapse, the numerical solution shows increasing distortion of the kink near the origin $r = 0$, which is not mirrored in the modulation solution as it is based on a fixed trial function of the 1D sine-Gordon equation kink. The equivalent comparison using the modulation theory of the present work is shown in Fig. 5. As expected, the present results agree with the previous work of Samuelsen (1979) as they are the same in this limiting case.

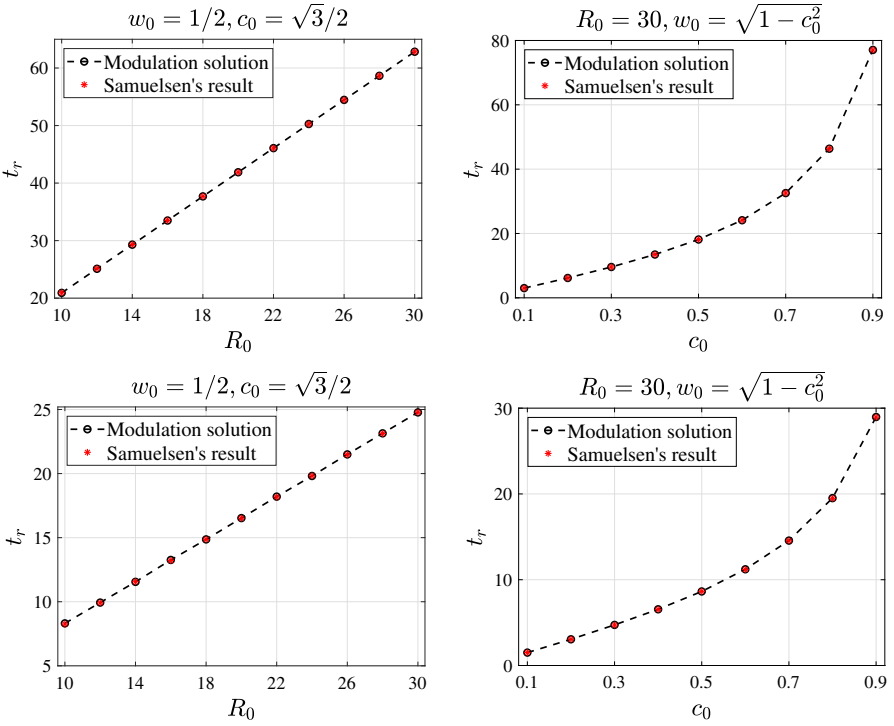


**Fig. 6** Return time for radially symmetric kinks for the 2D sine-Gordon equation. (left) Fixed initial conditions (27) with $w_0 = 1/2$, $c_0 = \sqrt{3}/2$ and $R_0$ varying from 10 to 30 with the step size $\Delta R_0 = 3$. (right) Fixed $R_0 = 30$ and $c_0 = \sqrt{1 - w_0^2}$ varying from 0.1 to 0.9 with the step $\Delta c_0 = 0.1$. The upper and lower panels are for the 2D and 3D sine-Gordon equations, respectively

## 4.2 Energy Conserving System with No Loss

### 4.2.1 Return Time

In this subsection, we compute the times $t_r$ at which the kink wave returns as a function of the initial radius $R_0$ and width $w_0$ given by (27). These return times are also compared with the analytical results of Christiansen and Olsen (1979); Samuelsen (1979). For the first comparisons, we fix $c_0 = \sqrt{3}/2$ and vary $R_0$ from 10 to 30 with the step $\Delta R_0 = 3$, while in the second set, we fix $R_0 = 30$ and vary $c_0$ from 0.1 to 0.9 with the increasing step $\Delta c_0 = 0.1$. These comparisons are shown in Fig. 6. It can be seen that there is excellent agreement between the returning times given by modulation theory and the predictions of Christiansen and Olsen (1979) and Samuelsen (1979).

### 4.2.2 Full Comparison of the Modulation Solutions with Numerical Solutions

We now compare modulation solutions of the modulation equations of Sect. 2.3 with full numerical solutions. Again, we use the initial conditions (27) for the modulation

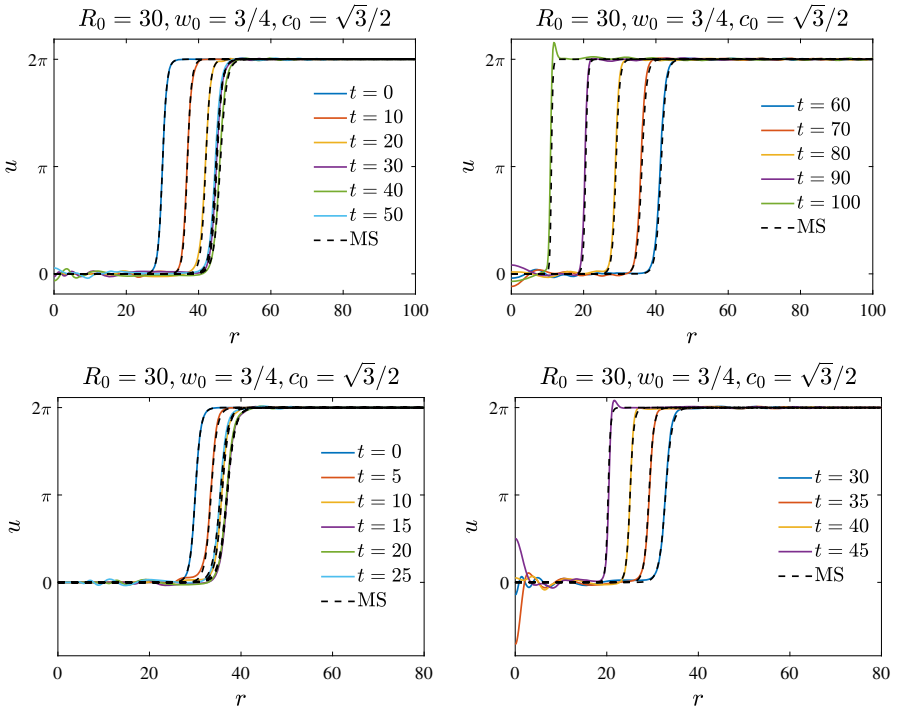


**Fig. 7** Comparison between modulation and numerical solutions for the initial condition (10). The numerical and modulation solutions at different time instants are shown in subfigures on the left and then on the right. The parameters for the initial condition (27) are shown in the subfigures. The upper and lower panels show solutions of the 2D and 3D sine-Gordon equations, respectively

equations. Substituting the modulation solution into the solution ansatz (10), the full ring-shaped kink wave is obtained and can be compared with full numerical solutions, as in Fig. 5. It can be seen that there is excellent agreement between the modulation and numerical solutions up to return, and after return until the kink approaches the origin and the point of collapse. The numerical solution shows that the kink undergoes deformation as it approaches collapse, particularly for the 3D case of the right hand figure. The modulation theory solution cannot be expected to give an adequate approximation to the solution evolution as collapse is approached as it is based on the fixed profile (10). The issue of a suitable trial function which can encompass both the self-similar evolution for return and then the approach to collapse, as well as the deformation of the kink on collapse, needs to be addressed in future work. We see from Fig. 5 that the ring-shaped kink recovers almost exactly its form after return. This property was partly reported and justified by the modulation theory (Le and Nguyen 2015) and a heuristic approach (Nguyen 2016). The current modulation theory reinforces the explanation for this return behaviour.

To show the advantage of the current modulation solution over that of previous work (Samuelsen 1979) based on a restricted trial function, we use the initial condition, (10), so that $w(0) \neq \sqrt{1 - [R'(0)]^2}$, which is not encompassed by the work of Samuelsen

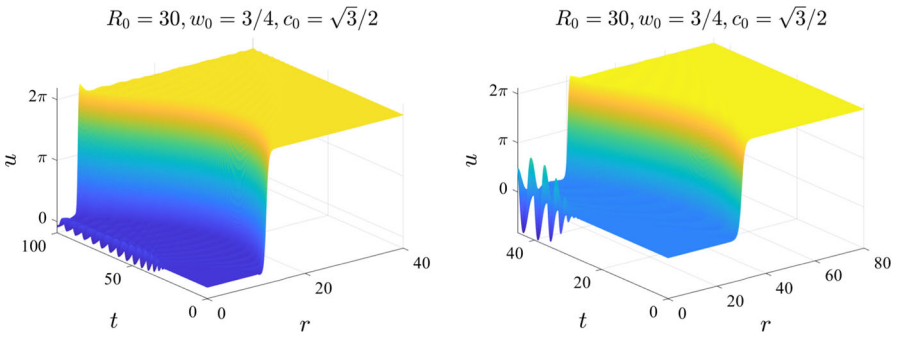


**Fig. 8** Evolution of a radially symmetric kink wave in 2D (left) and 3D (right). The parameters for the initial condition (27) are shown in the subfigures

(1979).[1] For illustration, Fig. 7 shows comparisons for the initial conditions (10) with $w_0 = 3/4$, $c_0 = \sqrt{3}/2$ and $R_0 = 30$. The comparisons between the full numerical and modulation solutions are shown for both the 2D and 3D sine-Gordon equations. Again, there is excellent agreement in both dimensions. In contrast to the specialized cases of Figs. 4 and 5 for which the initial condition is an exact kink solution of the 1D sine-Gordon equation, the modulation solutions show significant deviations from the numerical solutions in the tails of the kink. This is due to the initial condition shedding dispersive radiation to try to settle to an exact kink solution (Whitham 1974). In addition, the 3D kink shows significant distortion as it approaches the origin and collapse, more than that displayed in Figs. 4 and 5. Figure 8 shows the evolution of 2D and 3D kinks for the initial conditions of Fig. 7. The significant generation of radiation as the kinks approach the origin and collapse is clear.

Let us consider the specific initial conditions

$$R_0 = 30, \quad c_0 = \sqrt{3}/2, \quad w_0 = 1/2 \tag{42}$$

for both the 2D and 3D cases. Note that, these values guarantee $w_0 = \sqrt{1 - c_0^2}$, so that the initial condition corresponds to the exact kink solution of the 1D sine-Gordon equation and also recovers the initial condition considered in Christiansen and Olsen (1979); Samuelsen (1979). The numerical solution of the modulation equations (23) compared with the solution of Samuelsen (1979) is shown in Fig. 9 for the cylindrically symmetric (2D) and spherically symmetric cases (3D). It can be seen that the modulation solutions for both the position $R(t)$ and width $w(t)$ are in agreement, except for small, high-frequency oscillations in the kink width $w(t)$ as given by the current modulation theory, but not by the work of Samuelsen (1979). The position of the kink $R(t)$ increases with time, until the kink is reflected and returns, as found in previous work (Christiansen and Olsen 1979; Samuelsen 1979). These small, high-frequency width oscillations are due to the width being free to evolve independently

[1] It is not possible to perform any meaningful comparisons with the solution form given by Samuelsen (1979) as it does not allow this more general initial condition.

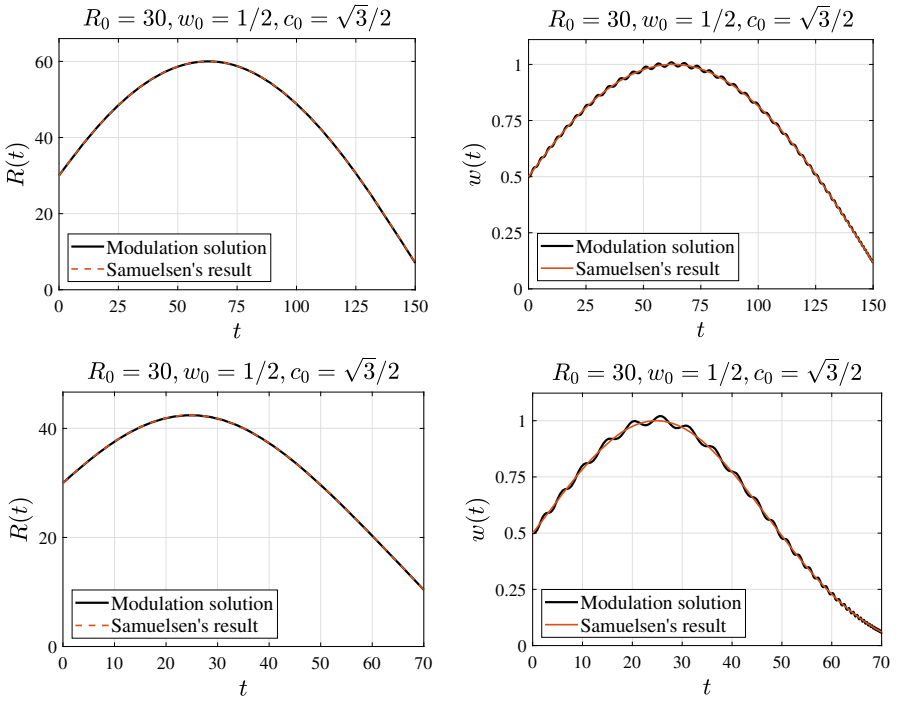


**Fig. 9** Modulation solutions (black lines) vs. Samuelsen's solutions (red lines) for propagation of ring-shaped kink for 2D and 3D sine-Gordon equations. The upper panel of figures corresponds to the 2D wave and the lower panel to the 3D wave

of the position so that it can undergo small scale adjustments. Samuelsen's solution gives the average of the modulation solution width over its internal oscillation period.

These small-scale, high-frequency width oscillations are present in full numerical solutions of the sine-Gordon equation. The width was computed from the numerical solution in the following manner. Let $\Delta u$ be a change in the solution of the sine-Gordon equation. We then define the position $r_1$ and $r_2$ such that

$$u(r_1, t) = \pi - \Delta u = u_1, \quad u(r_2, t) = \pi + \Delta u = u_2, \tag{43}$$

symmetric about the mid-point of $u$, where the expression for $u(r, t)$ is given by the ansatz (10). We note from Figs. 4, 5, 6 and 7 that this kink ansatz is a good approximation to the full numerical solution. Then, we have

$$u_j = 4 \arctan e^{-\frac{r_j - R(t)}{w(t)}}, \quad j = 1, 2 \quad \Rightarrow \quad w(t) = \frac{r_2 - r_1}{\ln[\tan(u_2/4)] - \ln[\tan(u_1/4)]}. \tag{44}$$

Let us now make comparisons between the modulation solutions and numerical solutions for the initial conditions (i) $R_0 = 30, c_0 = \sqrt{3}/2, w_0 = 1/2$ and (ii) $R_0, c_0 = \sqrt{3}/2, w_0 = 3/4$ for only the width parameter $w(t)$ using $\Delta u = \pi/4$. In Fig. 10, this numerical width is compared with the corresponding modulation solution

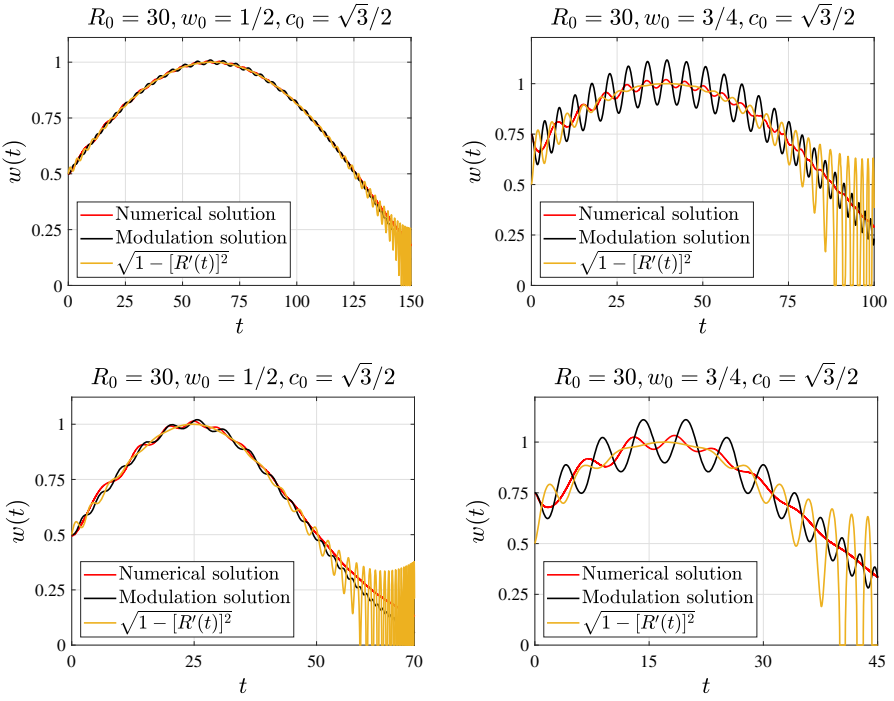


**Fig. 10** Numerical comparison justifying the oscillations in the width parameter $w(t)$. The results in the upper panel and lower panel are, respectively, for the ring-shaped kinks governed by the 2D sine-Gordon equation (upper panel) and the 3D sine-Gordon equation (lower panel)

as well as the time-dependent function $\gamma(t) = \sqrt{1-[R'(t)]^2}$, where $R(t)$ is also the modulation solution. Note that, this comparison requires $|R'(t)| \leq 1$. The full modulation theory of the present work is then a generalization to encompass the case $|R'| > 1$ of Samuelsen (1979). The figure shows the results for both the 2D (upper panel) and 3D (lower panel) sine-Gordon equations. The function $\gamma(t)$ is inspired by the 1D kink relation assumed in the work of Samuelsen (1979). It is clear that the width oscillations are also present in the numerical solution, as predicted by the current modulation theory. The small-scale width oscillations greatly increase in amplitude when the initial condition is not a 1D kink, $w_0 \neq \sqrt{1-c_0^2}$. As the kink approaches collapse, $\gamma(t)$ shows large amplitude oscillations of decreasing period. Modulation theory and numerical solutions differ in the amplitude of the width oscillations, but essentially agree on the period of these oscillations. In general, modulation theory gives better predictions for the width oscillations for the 3D sine-Gordon equation.

Let us now perform one more numerical experiment for which we set the initial shape of the solution as in the trial function $(10)_1$ at $t = 0$, but with zero initial velocity, that is $u_t(r, 0) = 0$, $w_0 = 1$ and $c_0 = 0$. This corresponds to the initial conditions for the parameters $w(t)$ and $R(t)$, $w'(0) = 0$ and $R'(0) = 0$. The solutions for both the 2D and 3D sine-Gordon equations are shown in Fig. 11. It is seen that the kink does not propagate forward, but returns to the origin $r = 0$ immediately.

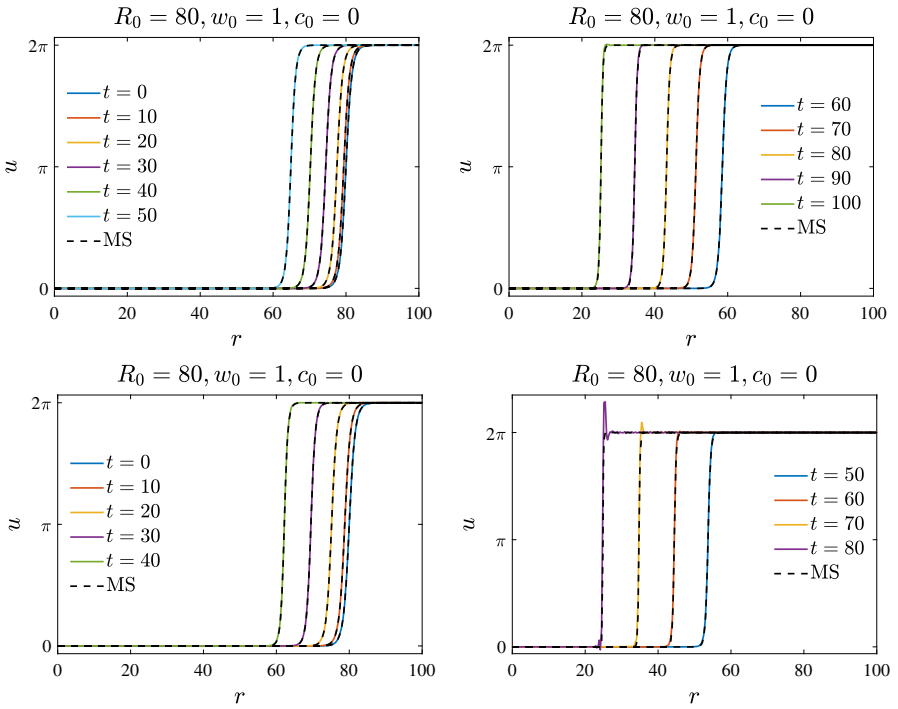


**Fig. 11** Comparisons between modulation and numerical solutions for the initial condition (10): (upper) 2D sine-Gordon equation, (lower) 3D sine-Gordon equation. The parameters for the initial condition (27) are shown in the subfigures

In summary, the comparisons of this section show that the modulation theory of the present work can be applied to a wide range of initial conditions of the type (27), which encompass initial conditions which are not 1D sine-Gordon equation kinks, unlike previous work.

### 4.3 Energy Dissipative System

These comparisons for the 2D and 3D sine-Gordon equations can be extended to the dissipative sine-Gordon Eq. (6) with $\beta \neq 0$. Again, it is found that the modulation theory gives excellent agreement with numerical solutions. For these comparisons, we set the viscosity coefficient in (6) to $\beta = 1/10$. To this end, we take two initial conditions (i) $w_0 = 1/2$, $c_0 = \sqrt{3}/2$ and $R_0 = 30$ and (ii) $w_0 = 3/4$, $c_0 = \sqrt{3}/2$ and $R_0 = 70$. The parameters $w_0$ and $c_0$ in the first case satisfy the 1D kink condition $c_0 = \sqrt{1 - w_0^2}$, while this is not the case for the second initial condition. The comparisons between the modulation and the numerical solutions are shown in Fig. 12. Again, the ring-shaped kink expands for a finite time before it returns. However, we do not observe strong dispersion effects on the two stable levels $u = 0$ and $u = 2\pi$ in the case $w_0 \neq \sqrt{1 - c_0^2}$ as for the kink solution governed by the non-dissipated sine-

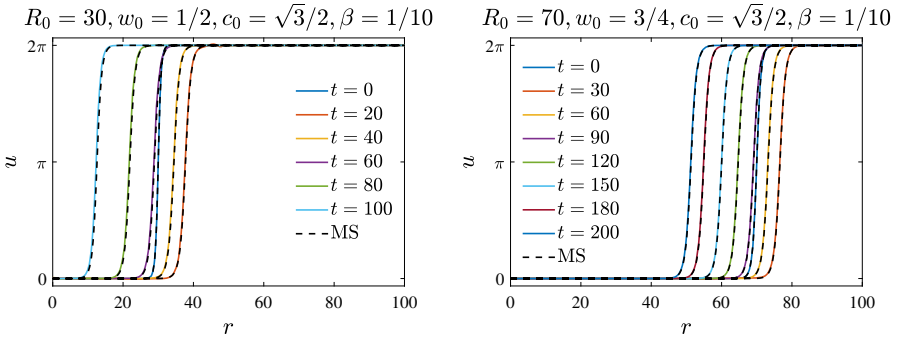


**Fig. 12** Comparison between modulation and numerical solutions of the 2D dissipative sine-Gordon equation with the damping coefficient $\beta = 1/10$. The parameters defined in the initial conditions (27) are given in the two subfigures corresponding to two different numerical experiments

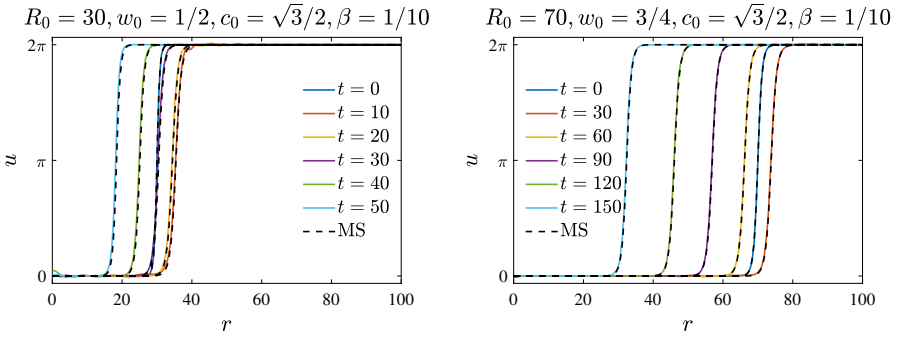


**Fig. 13** Comparison between modulation and numerical solutions for the 3D dissipative sine-Gordon equation with the damping coefficient $\beta = 1/10$. The parameters defined in the initial conditions (27) are given in the two subfigures corresponding to the two different numerical experiments

Gordon equation, see Fig. 8. This reduced role of shed radiation is due to it being rapidly damped as $\beta \neq 0$. Similar numerical results for the 3D sine-Gordon equation are shown in Fig. 13, with again the role of shed radiation greatly reduced due to the loss over the lossless case.

## 5 Conclusion

In the present work, we have developed a modulation theory based on a variational approximation to study ring-shaped kinks governed by two-dimensional and three-dimensional sine-Gordon equations with damping. Although the derived system of modulation equations for the wave parameters is involved, it can be solved numerically with the symbolic software MATHEMATICA Wolfram Research (2020) with appropriate initial conditions for the involved wave parameters. The developed modulation theory generalizes the previous heuristic results reported in Christiansen and Olsen (1979); Samuelsen (1979) in two key aspects: (i) the new theory does not set the relation

between the velocity and the width of the kink throughout the evolution of the wave, (ii) the theory can predict the evolution of waves with damping. The modulation solutions were compared with direct numerical solutions, with excellent agreement found over a wide range of initial parameter values, both with and without damping. This confirms the advantage of the present modulation theory over the existing results reported by Christiansen and Olsen (1979) and Samuelsen (1979). We note that the present variational approximations can be applied to study ring-shaped kinks governed by other nonlinear dispersive wave equations, for instance Klein-Gordon equations.



## Appendix 1 Derivation of averaged Lagrangian and averaged Dissipation Densities

In this appendix, we derive expressions for the averaged Lagrangian $\mathcal{L}_d$ defined by (16) and the averaged dissipation densities $\mathcal{D}_d^R$ and $\mathcal{D}_d^w$ defined by (17). Note that, we suppress the explicit dependence of $\mathcal{L}_d, \mathcal{D}_d^R, \mathcal{D}_d^w$ and $a, b$ on their arguments, namely $R(t), w(t), R'(t)$ and $w'(t)$. Let us start by calculating $\mathcal{L}_d$ by separating it into three terms as follows

$$\mathcal{L}_d = \mathcal{L}_d^{\text{kin}} - \mathcal{L}_d^{\text{int}} - \mathcal{L}_d^{\text{pot}}, \tag{45}$$

where $\mathcal{L}_d^{\text{kin}}$, $\mathcal{L}_d^{\text{int}}$ and $\mathcal{L}_d^{\text{pot}}$ correspond to the kinetic energy, interaction energy and potential field $\phi(u) = 1 - \cos u$ and are given by

$$\mathcal{L}_d^{\text{kin}} = \frac{1}{2}\int_0^\infty u_t^2 r^{d-1}\mathrm{d}r, \quad \mathcal{L}_d^{\text{int}} = \frac{1}{2}\int_0^\infty u_r^2 r^{d-1}\mathrm{d}r, \quad \mathcal{L}_d^{\text{pot}} = \int_0^\infty (1-\cos u)\mathrm{d}r. \tag{46}$$

By using the explicit expression of $u_t$ given in (11) in $\mathcal{L}_d^{\text{kin}}$ and $\mathcal{L}_d^{\text{int}}$, we obtain

$$\begin{aligned}
\mathcal{L}_d^{\text{kin}} &= \frac{2}{w^4}\int_0^\infty \operatorname{sech}^2\left(\frac{r-R}{w}\right)(ar+b)^2 r^{d-1}\mathrm{d}r \\
&\quad \frac{2}{w^4}\left[a^2 G_{d+1}(R,w) + 2abG_d(R,w) + b^2 G_{d-1}(R,w)\right] \\
\mathcal{L}_d^{\text{int}} &= \frac{2}{w^2}\int_0^\infty \operatorname{sech}^2\left(\frac{r-R}{w}\right) r^{d-1}\mathrm{d}r = \frac{2}{w^2}G_{d-1}(R,w),
\end{aligned} \tag{47}$$

where $G_j(R,w) = \int_0^\infty r^j \mathrm{sech}^2\left(\frac{r-R}{w}\right)\mathrm{d}r$. To compute $G_j(R,w)$, we use the change of variable $\xi = (r-R)/w$ so that

$$G_j(R,w) = \int_{-R/w}^{\infty} w(w\xi + R)^j \mathrm{sech}^2\xi \mathrm{d}\xi = w\sum_{k=0}^{j} \mathrm{C}_j^k \int_{-R/w}^{\infty} \xi^k \mathrm{sech}^2\xi \mathrm{d}\xi\, w^k R^{j-k}, \tag{48}$$

where

$$C_j^k = \frac{j!}{k!(j-k)!} \tag{49}$$

are the binomial coefficients. In this manner, the derivation of explicit expressions for $G_j$ is reduced to computing the anti-derivatives $f_k(\xi) = \int \xi^k \mathrm{sech}^2\xi \mathrm{d}\xi$ for $k = 1, \ldots, 4$. These anti-derivatives can be obtained by the symbolic software MATHEMATICA Wolfram Research (2020). However, the results are lengthy and not presented here. By denoting

$$N_k(R/w) = \lim_{\xi\to\infty} f_k(\xi) - f_k(-R/w), \quad k = 1, \ldots, 4, \tag{50}$$

we arrive at

$$G_j(R,w) = w\left[\sum_{k=0}^{j} \mathrm{C}_j^k w^k N_k(R/w) R^{j-k}\right], \quad j = 1, \ldots, 4. \tag{51}$$

Even though the expressions for $N_k(R/w)$ are rather complicated, the final expressions for $G_j(R/w)$ are simple, as in (20). With the solution ansatz (10), we establish the relation $1 - \cos u = 2\mathrm{sech}^2\left(\frac{r-R}{w}\right)$ and thus

$$\mathcal{L}_d^{\mathrm{pot}} = 2\int_0^\infty \mathrm{sech}^2\left(\frac{r-R}{w}\right) r^{d-1}\mathrm{d}r = 2G_{d-1}(R,w). \tag{52}$$

By substituting (47) and (52) into (45), we arrive at equation (18).

The derivation of $\mathcal{D}_d^R$ and $\mathcal{D}_d^w$ can be performed in a similar manner. Differentiating the solution ansatz (10) with respect to $R$ and $w$ gives

$$\frac{\partial u}{\partial R} = -\frac{2}{w}\mathrm{sech}\left(\frac{r-R}{w}\right), \quad \frac{\partial u}{\partial w} = -\frac{2(r-R)}{w^2}\mathrm{sech}\left(\frac{r-R}{w}\right). \tag{53}$$

Substituting these expressions and the derivative $u_t$ given by (11) into the definition (17) of the averaged dissipation densities, we arrive at

$$\begin{aligned}\mathcal{D}_d^R &= \beta\int_0^\infty u_t\frac{\partial u}{\partial R}r^{d-1} = \beta\frac{4}{w^3}\int_0^\infty \operatorname{sech}^2\left(\frac{r-R}{w}\right)(ar+b)r^{d-1}\mathrm{d}r,\\ &= \beta\frac{4}{w^3}\big[a\,G_d(R,w)+b\,G_{d-1}(R,w)\big],\\ \mathcal{D}_d^w &= \beta\int_0^\infty u_t\frac{\partial u}{\partial w}r^{d-1} = \beta\frac{4}{w^4}\int_0^\infty \operatorname{sech}^2\left(\frac{r-R}{w}\right)(r-R)(ar+b)r^{d-1}\mathrm{d}r,\\ &= \beta\frac{4}{w^4}\big[a\,G_{d+1}(R,w)+(b-aR)G_d(R,w)-bR\,G_{d-1}(R,w)\big].\end{aligned} \tag{54}$$

The latter results agree with those given by (22).

## References


Adkins, G.S., Nappi, C.R., Witten, E.: The skyrme model with pion masses. Nucl. Phys. B **228**, 552–566 (1983)

Anderson, D.: Variational approach to nonlinear pulse propagation in optical fibers. Phys. Rev. A **27**, 3125–3145 (1983)

Bathe, K.: Finite Element Procedures, 2nd edn. Klaus-Jurgen Bathe, Berlin (2014)

Christiansen, P.L., Olsen, O.H.: Ring-shaped quasi-soliton solutions to the two- and three-dimensional sine-gordon equation. Phys. Scr. **20**, 531–538 (1979)

Wolfram Research, Inc. Mathematica, Version 12.2. Champaign, IL, (2020)

Kath, W.L., Smyth, N.F.: Soliton evolution and radiation loss for the nonlinear schrödinger equation. Phys. Rev. E **51**, 1484–1492 (1995)

Kivshar, Y.S., Malomed, B.A.: Dynamics of solitons in nearly integrable systems. Rev. Mod. Phys. **61**(4), 763 (1989)

Kudryavtsev, A., Piette, B., Zakrzewski, W.J.: Mesons, baryons and waves in the baby skyrmion model. Euro. Phys. J. C **1**, 333–341 (1998)

Lamb, G.L.: Elements of Soliton Theory. Wiley, New York (1980)

Le, K.C., Nguyen, L.T.K.: Slope modulation of ring waves governed by two-dimensional sine-gordon equation. Wave Motion **55**, 84–88 (2015). (**6**)

Le, K.C., Nguyen, L.T.K.: Slope modulation of waves governed by sine-gordon equation. Commun. Nonlinear Sci. Numer. Simul. **18**, 1563–1567 (2013)

Malomed, B.: Variational methods in nonlinear fiber optics and related fields. Prog. Opt. **43**, 71–193 (2002)

McLaughlin, D.W., Scott, A.C.: Perturbation analysis of fluxon dynamics. Phys. Rev. A **18**(4), 1652 (1978)

Minzoni, A.A., Smyth, N.F., Worthy, A.L.: Evolution of two dimensional standing and travelling breather solutions for the sine-gordon equation. Physica D **189**, 167–187 (2004)

Minzoni, A.A., Smyth, N.F., Worthy, A.L.: Pulse evolution for a two-dimensional sine-gordon equation. Physica D: Nonlinear Phenomena **159**, 101–123 (2001)

Neu, J.C.: Kinks and the minimal surface equation in minkowski space. Physica D **43**, 421–434 (1990)

Nguyen, L.T.K.: A numerical scheme and some theoretical aspects for the cylindrically and spherically symmetric sine-gordon equations. Commun. Nonlinear Sci. Numer. Simul. **36**, 402–418 (2016)

Piette, B., Zakrzewski, W.J.: Metastable stationary solutions of the radial $d$-dimensional sine-gordon model. Nonlinearity **11**, 1103–1110 (1998)

Samuelsen, M.R.: Approximate rotationally symmetric solutions to the sine-gordon equation. Phys. Lett. A **74**, 21–22 (1979). (**10**)

Smyth, N.F., Worthy, A.L.: Soliton evolution and radiation loss for the sine-gordon equation. Phys. Rev. E **60**, 2330–2336 (1999)

Whitham, G.B.: A general approach to linear and non-linear dispersive waves using a lagrangian. J. Fluid Mech. **22**, 273–283 (1965)

Whitham, G.B.: Linear and Nonlinear Waves. Wiley, New York (1974)